ACCOUNTS of chemical research

Article

Cite This: Acc. Chem. Res. 2019, 52, 1409−1418

pubs.acs.org/accounts

What Your Crystal Structure Will Not Tell You about Enzyme Function

Thomas C. Pochapsky*[,†,‡] and Susan Sondej Pochapsky[†]

[†]Department of Chemistry and [‡]Department of Biochemistry, Brandeis University 415 South Street, Waltham, Massachusetts 02454, United States

CONSPECTUS: Enzyme function requires that enzyme structures be dynamic. Substrate binding, product release, and transition state stabilization typically involve different enzyme conformers. Furthermore, in multistep enzyme-catalyzed reactions, more than one enzyme conformation may be important for stabilizing different transition states. While X-ray crystallography provides the most detailed structural information of any current methodology, X-ray crystal structures of enzymes capture only those conformations that fit into the crystal lattice, which may or may not be relevant to function. Solution nuclear magnetic resonance (NMR) methods can provide an alternative approach to characterizing enzymes under nonperturbing and controllable conditions, allowing one to identify and localize dynamic processes that are important to function. However, many enzymes are too large for standard approaches to making sequential resonance assignments, a critical first step in analyzing and interpreting the wealth of information inherent in NMR spectra.

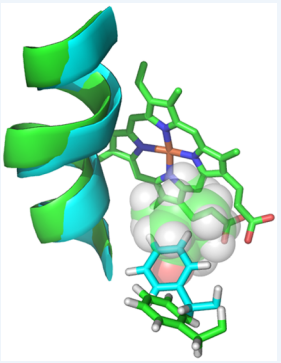

This Account describes our long-standing NMR-based research into structural and dynamic aspects of function in the cytochrome P450 monooxygenase superfamily. These heme-containing enzymes typically catalyze the oxidation of unactivated C−H and C═C bonds in a multitude of substrates, often with complete regio- and stereospecificity. Over 600 000 genes in GenBank have been assigned to P450s, yet all known P450 structures exhibit a highly conserved and unique fold. This combination of functional and structural conservation with a vast substrate clientele, each substrate having multiple possible sites for oxidation, makes the P450s a unique target for understanding the role of enzyme structure and dynamics in determining a particular substrate−product combination. P450s are large by solution NMR standards, requiring us to develop specialized approaches for making sequential resonance assignments and interpreting the spectral changes that occur as a function of changing conditions (e.g., oxidation and spin state changes, ligand, substrate or effector binding). Solution conformations are characterized by the fitting of residual dipolar couplings (RDCs) measured for sequence-specifically assigned amide N−H correlations to alignment tensors optimized in the course of restrained molecular dynamics (MD) simulations. The conformational ensembles obtained by such RDC-restrained simulations, which we call "soft annealing", are then tested by site-directed mutation and spectroscopic and activity assays for relevance. These efforts have gained us insights into cryptic conformational changes associated with substrate and redox partner binding that were not suspected from crystal structures, but were shown by subsequent work to be relevant to function. Furthermore, it appears that many of these changes can be generalized to P450s besides those that we have characterized, providing guidance for enzyme engineering efforts. While past research was primarily directed at the more tractable prokaryotic P450s, our current efforts are aimed at medically relevant human enzymes, including CYP17A1, CYP2D6, and CYP3A4.

Dear Enzymologist,

It is time we had a talk. Yes, "a picture is worth a thousand words", and "seeing is believing". The crystal structure of your enzyme exposed the secrets of the active site, identified critical residues, and let you dream of inhibitor design and enzyme engineering. You love your structure, but you are troubled. Why does substrate bind in the wrong orientation or not at all? What about those allosteric, synergistic, and antagonistic effects that you see in your assays about which the structure is mum? You screened potential inhibitors by the thousands against the structure, but either hits led to nothing, or when you crystallized the resulting complex, it did not look at all like what was predicted.

Here is the problem: Enzymes are dynamic and occupy multiple conformations at their working temperatures. But the crystallization process is also a purification: Only those conformers that fit into the growing lattice will be accepted. Unfortunately, there is no way of knowing *a priori* whether the crystallographic conformation is relevant to catalysis or, if it is, which step in a reaction pathway it represents.

Nuclear magnetic resonance (NMR) can provide insights into solution structure and dynamics when static methods are insufficient. NMR allows one to control variables such as composition, temperature, solvent, pH, and other factors affecting dynamic processes and conformations in a (relatively) nonperturbing environment. However, while NMR analysis of proteins 10−30 kDa in size is straightforward, enzymes are often

Received: February 7, 2019
Published: April 29, 2019

DOI: 10.1021/acs.accounts.9b00066
Acc. Chem. Res. 2019, 52, 1409−1418

larger than this, and much hard work is needed in order to reap the benefits that NMR promises.

Our group's research for the last 30 years has been aimed at using NMR to improve our understanding of enzyme structure and dynamics and to refine the techniques we use in order to accomplish that goal. We have focused on cytochrome P450 monooxygenases, heme-containing enzymes that typically catalyze the hydroxylation of unactivated C−H bonds (Scheme 1), although they can also function as epoxidases and demethylases and in the catalysis of oxidative couplings.

Scheme 1

$$R\text{-}H + O_2 + 2\,e^- + 2\,H^+ \rightarrow R\text{-}OH + H_2O$$

The remarkable structural conservation combined with the vast array of substrate/product combinations exhibited by the P450 superfamily makes it an ideal target for understanding molecular recognition in biological systems.[1] In this report, we will attempt a comprehensive description of the insights we have gained into P450 structure and dynamics, as well as the methods we have used or developed along the way.

EFFECTOR FUNCTION IN MONOOXYGENASES: THE PUTIDAREDOXIN-CYTOCHROME P450$_{cam}$ COUPLE

We began our efforts by focusing on the cytochrome P450$_{cam}$ (CYP101A1) reaction cycle. CYP101A1 catalyzes the 5-*exo* hydroxylation of *d*-camphor, the first step in camphor catabolism by the soil bacterium *Pseudomonas putida*.[2] CYP101A1 was the first P450 for which a crystal structure was determined,[3] and most of what is known about the mechanism of O_2 activation by P450s has been learned with this enzyme. The reaction catalyzed by the 46.7 kDa CYP101A1 (Figure 1) is remarkable for its efficiency, specificity, and regulation. The enzyme is better than 99% efficient in its use of reducing equivalents, and camphor hydroxylation is completely regio- and stereospecific. The reaction requires two additional proteins, putidaredoxin reductase (PdR), that oxidizes NADH to provide the needed electrons, and the 11.6 kDa Fe_2S_2-containing putidaredoxin (Pdx), which acts as an electron shuttle between PdR and CYP101A1.

Upon *d*-camphor binding, the heme iron in CYP101A1 shifts from ferric low spin ($S = 1/2$) to the high spin ($S = 5/2$) form,[4] shifting the reduction potential from −303 mV to −173 mV. As the potential of reduced Pdx (Pdx^r) is −240 mV, electron transfer from Pdx^r to high spin CYP101A1 is nearly iso-energetic ($K_{eq} = \sim 2.3$), maximizing the rate of electron transfer. Substrate binding is thus an on−off switch; Pdx^r does not reduce CYP101A1 unless substrate is bound. Upon reduction, the heme iron can ligate O_2 required for turnover. However, Pdx is not merely a reductant but also acts as an effector for turnover. In fact, the first reduction of CYP101A1 can be done by any reductant with a sufficiently negative potential. In the absence of Pdx, however, the O_2−CYP101A1−substrate complex (CYP^r−S−O_2) slowly decomposes to superoxide and CYP^o−S.[5] Binding of Pdx^r drives a rate determining conformational change in CYP^r−S−O_2, so the Pdx^r−CYP^r−S−O_2 complex is the enzymatically competent species for turnover. But what is the nature of that complex, and what is the conformational change that Pdx binding drives?

Pdx Structure and Dynamics

A necessary first step was to determine the structure of Pdx. The CYP101A1 structure had been obtained in a number of forms by the late 1980s, but Pdx had defied crystallographic analysis, nor were there any related ferredoxin structures available. Could a Pdx structure be obtained by NMR? By 1989, homonuclear (i.e., ^{1}H, ^{1}H) two-dimensional (2D) NMR methods had advanced sufficiently that the answer was a qualified yes. Amino acid ^{1}H spin systems could be established using through-bond experiments such as TOCSY and COSY, and the spin systems could be sequentially and structurally connected using through-space (nuclear Overhauser effect, NOE) correlations. We published preliminary ^{1}H sequential resonance assignments for oxidized Pdx (Pdx^o), along with evidence for an extensive β-sheet structure in 1991.[6] By 1994, graduate researcher Xiaomei Ye had accumulated sufficient NOEs to publish a structure of Pdx^o,[7] the first *de novo* metalloprotein structure to be solved by NMR. Paramagnetic broadening of ^{1}H resonances within a ∼8 Å radius of the Fe_2S_2 cluster required us to model the cluster into the structure, and while Sophia Kazanis was able to prepare a diamagnetic form of Pdx by reconstitution with gallium salts,[8,9] we were nonetheless relieved when a crystal structure for the

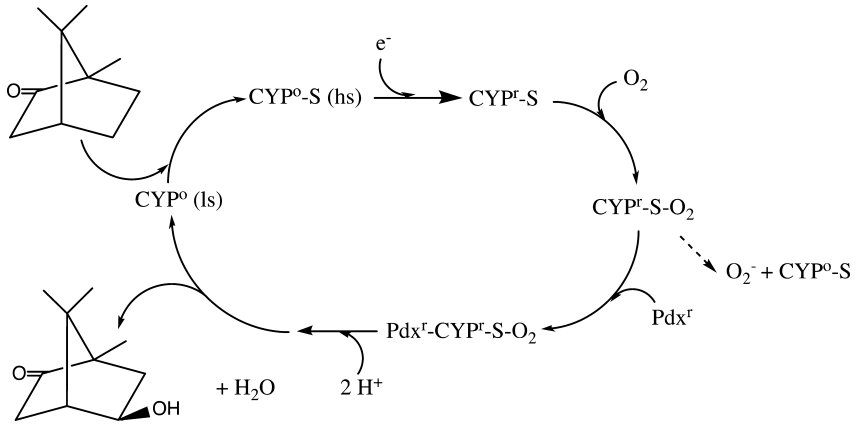

Figure 1. Catalytic cycle of CYP101A1. Binding of *d*-camphor (upper left) induces a spin state shift from low spin (ls) to high-spin (hs) permitting the first electron transfer. O_2 binds to the reduced enzyme, and binding of Pdx generates the catalytically competent complex to produce 5-*exo*-hydroxycamphor (lower left). In the absence of Pdx, the O_2 complex decomposes to superoxide and the enzyme−substrate complex (dotted line, right). See text for details.

DOI: 10.1021/acs.accounts.9b00066
Acc. Chem. Res. 2019, 52, 1409−1418

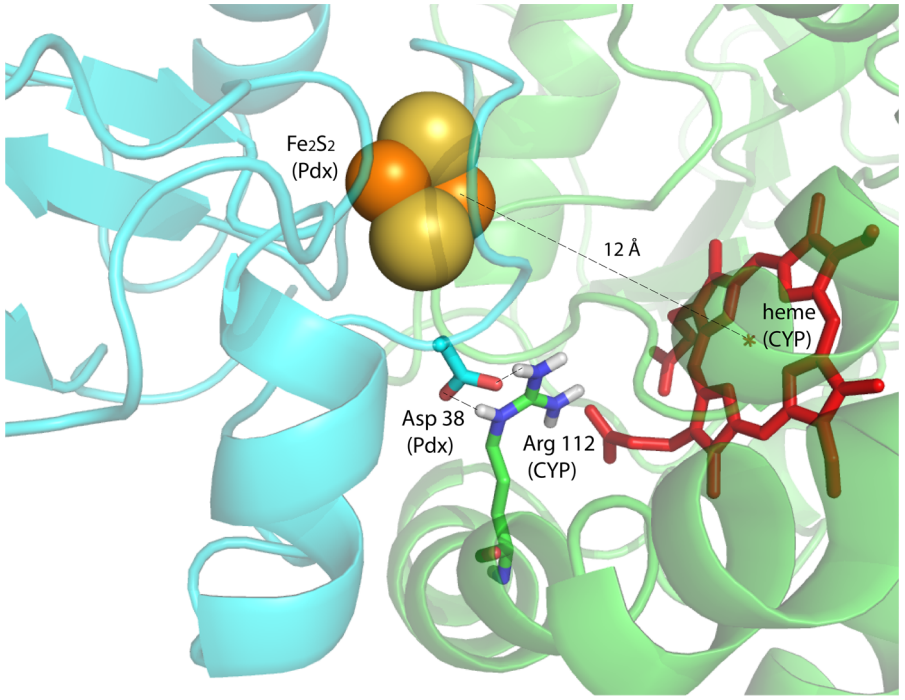

Figure 2. Close-up of the interface between complexed Pdx and CYP101A1 proposed in ref 13. The Pdx polypeptide is shown in cyan, CYP101A1 in green. The 12 Å vector between the heme iron and Fe_2S_2 iron adjacent to the surface is shown as a dotted line, as are salt bridge interactions between Asp38 and Arg112. (PDB-format file available from the authors upon request.)

related adrenodoxin was published,[10] showing that our modeling of the metal center was accurate.

Having in hand our NMR-derived structure for Pdx^o, it was an irresistible temptation to propose a model for the Pdx−CYP complex. Residues on both proteins had been identified as important for complexation, Arg109 and Arg112, both on the C-helix of CYP101A1, and the Pdx C-terminal Trp106.[11,12] We assumed that positively charged Arg residues would interact with carboxylates on Pdx, that the indole of Trp106 would interact with hydrophobic residues on the surface of CYP101A1, and that the redox centers of both proteins would be close to each other, leading us to the model shown in close-up in Figure 2.[13] The most predictive feature of this model was the appearance of a salt bridge between Arg112 on CYP101A1 and Asp38 on Pdx. Subsequent mutagenesis showed that Asp38 is important in mediating complexation,[14] and recently, crystallographic structures of the Pdx−CYP101A1 complex confirmed the interaction.[15,16]

This picture was far from complete, however. The relevant complex is between reduced Pdx (Pdx^r) and $CYP^r{-}S{-}O_2$. We found that reduction of Pdx involved significant changes in local dynamics, particularly near the C-terminal Trp106 and around the metal center.[17] Using ^1H,^{15}N HSQC experiments, we showed that amide proton exchange in multiple regions of Pdx is slowed upon reduction.[18] A painstaking selective ^{15}N, ^{13}C double labeling effort by Nitin Jain allowed us to assign backbone resonances in the vicinity of the Fe_2S_2 cluster of Pdx and directly link a contraction of the structure in the metal cluster binding loop upon reduction to the overall redox-dependent changes in dynamics.[19,20] We later showed that redox-dependent dynamics are not peculiar to Pdx but a general feature of related ferredoxins.[21]

The close coupling between oxidation state and dynamics in Pdx provided other insights. The formation of a Pdx−CYP101A1 complex stable enough to drive a conformational change would require "freezing" some degrees of freedom in Pdx, which comes at an entropy price. If some of that price was prepaid upon reduction, the enthalpy change upon complex formation might be sufficient to drive whatever conformational changes occur in CYP101A1. Furthermore, upon reoxidization, dissociation would be encouraged by the increased dynamics of Pdx^o, minimizing back electron transfer. It also rationalized our difficulties with Pdx crystallography. Pdx^o crystallizes readily, forming large black crystals we referred to as "the Borg" (*Star Trek* fans will understand the reference). "The Borg" diffracted immediately after insertion into the X-ray beam, but diffraction quality decreased rapidly upon continued X-ray exposure. As reduction causes contraction of the Pdx structure,[20] it was likely that photoelectron reduction increased the mobility of individual Pdx molecules, decreasing order in the crystal. More recently, crystallographic structures have been solved for Pdx that show redox-dependent conformational changes in the vicinity of the metal cluster.[22,23]

Pdx-Driven Changes in CYP101A1

Of course, Pdx structure and dynamics tells less than half of the story. For a complete picture, we needed to look at CYP101A1 directly. Fortunately, solution NMR methods improved rapidly during the 1990s, with the introduction of three-dimensional (3D) NMR experiments that allowed sequential ^1H, ^{15}N, and ^{13}C resonance assignments of the polypeptide without requiring NOE connectivity.[24] This gave us hope that the 46.7 kDa CYP101A1 might be tackled.

However, there were still challenges. The experiments we use for sequential assignments (HNCA, HN(CO)CA, HNCACB) are "there and back again" sequences: That is, coherence is first generated on the amide ^1H and passed via the ^{15}N to either the adjacent $^{13}C\alpha$ carbon (HNCA) or through the amide carbonyl to the $^{13}C\alpha$ of the preceding residue (HN(CO)CA). In HNCACB, the coherence is transferred a step further, to the

DOI: 10.1021/acs.accounts.9b00066
Acc. Chem. Res. 2019, 52, 1409−1418

Figure 3. NMR-derived solution structure of camphor-bound CYP101A1 (PDB entry 2L8M). Secondary structures are labeled as described by Poulos (ref 3). Heme is shown as sticks (background) and substrate *d*-camphor in the foreground as translucent space-filling spheres. Thus, the foreground is the distal (active site) side of the heme.

$^{13}C\beta$. After frequency labeling of the connected nuclei, coherence is returned to the amide ^{1}H for detection. The success of the experiment depends upon coherences being sufficiently long-lived that they can still be detected at the end of the sequence. ^{13}C spins with attached protons are particularly susceptible to rapid coherence loss, and coherence lifetimes get shorter with increasing molecular weight. This, combined with sheer spectral complexity, is the primary reason that NMR becomes more difficult as proteins get bigger.

In order for these experiments to work with CYP101A1, the density of ^{1}H spins present in the sample must be minimized. Besides uniform ^{15}N and ^{13}C labeling, then, the enzyme requires perdeuteration (u-^{2}H), replacing all (>99%) of the protons in the sample with deuterons. ^{2}H is much less efficient than ^{1}H in stimulating ^{13}C relaxation, and coherence lifetimes are increased sufficiently to allow "there and back again" experiments. Perdeuteration requires that growth media be prepared with $^{2}H_2O$, uniformly ^{13}C, ^{2}H labeled carbon sources, and salts lyophilized to remove $^{1}H_2O$. Needless to say, our standard expression strains are less than thrilled with the menu we provide and require "training" growths with increasing concentrations of $^{2}H_2O$ before we grow in the fully labeled (and expensive) media.

Protein produced in this fashion is *fully* perdeuterated, with ^{2}H present even at the amide positions, where ^{1}H is required for NMR. For proteins that can be unfolded/refolded in good yield, this problem is easily overcome. Sadly, P450s are notoriously resistant to this treatment, so we must rely on whatever $^{1}H/^{2}H$ exchange occurs during purification. Slow amide exchange, along with the presence of 35 prolines (which lack an amide NH) in the 414-residue CYP101A1, introduces multiple interruptions in the $^{1}H-^{15}N$-dependent assignment process. The paramagnetism of the heme further complicates the assignment process due to efficient relaxation of nearby protons.

To address these problems, we prepared a series of CYP101A1 samples containing type-selective ^{15}N labels for most amino acids. These samples were used to classify $^{1}H-^{15}N$ correlations by residue type, which were used as starting points for sequential assignments and to confirm tentative assignments. Another CYP101A1 sample was prepared with ^{13}C-Pro and (u-^{15}N) labeling. An HNCO experiment, requiring a $^{1}H-^{15}N$ correlation to be preceded by a ^{13}C carbonyl for detection, identified Pro−Xaa correlations. To avoid paramagnetic relaxation, most of our assignments were made for the diamagnetic reduced CO-bound CYP101A1 (CYP^{r}−S−CO).

By 2003, we had made sufficient progress to begin investigating Pdx−CYP interactions. Titrating Pdx^{r} into CYP^{r}−S−CO and monitoring by $^{1}H,^{15}N$ TROSY-HSQC,[25] we identified many CYP101A1 residues perturbed upon Pdx^{r} binding. While some perturbations were unsurprising, particularly in helix C of the P450 (Figure 2), we also saw changes in and near the active site, opposite from the proposed Pdx binding site on the proximal face (Figure 3). These included I helix residues adjacent to the heme, as well as residues in the B−B′ loop and B′ helices bordering what was assumed to be the entrance to the active site.[26] Based on these observations, we proposed a "doorstop" model for the effector activity of Pdx, in which the crystallographic conformation of CYP101A1 represented the "closed door" (and catalytically competent) form of the enzyme.[27] In solution, more open CYP conformers predominate, with less impeded active site access, but are not catalytically competent. The binding of Pdx would drive the formation of the closed form and permit turnover after the second electron transfer.[25]

A second titration series used (u-^{2}H)-Pdx^{r} and (u-^{2}H)-CYP^{r}−S−CO, so the most prominent ^{1}H NMR signals were those of *d*-camphor.[28] Ring current shifts were used to characterize the

DOI: 10.1021/acs.accounts.9b00066
Acc. Chem. Res. 2019, 52, 1409−1418

orientation of camphor in the active site with and without Pdx^r bound. Notably, the ^{1}H shifts of the three camphor methyl groups best fit the crystallographic orientation when Pdx is bound. In the absence of Pdx, camphor reorients so that the 5-*exo* C−H bond is too far from the heme iron for the observed regiochemistry.[28] We observed that the Pdx-driven conformational change in CYP101A1 is poised between slow and fast exchange on the ^{1}H shift time scale: Resonances moving more than ∼180 Hz during the titration show slow exchange behavior (two discrete signals for Pdx-free and -bound forms), while those moving less than ∼120 Hz are in fast exchange (a single signal moving through the titration course). We interpreted this as meaning that all of the Pdx-dependent perturbations were driven by the same event, taking place at a rate of ∼700 s^{-1} at half-saturation (∼2:1 Pdx/CYP). On the time scales of most protein motions, this rate is positively glacial. However, the *cis*−*trans* isomerization of an Xaa−Pro peptide bond can be this slow, so we looked for prolines in CYP101A1 that might trigger the conformational change. An obvious candidate was Pro89, at the beginning of the B′ helix, adjacent to the proposed active site access. In most crystallographic structures of CYP101A1, the Ile88−Pro89 bond is *cis*, resulting in the "closed door" active site, although a recent structure of the tethered Pdx−CYP101A1 complex shows the Ile88−Pro89 bond as distorted *trans*.[29] Mutation of Pro89 to Ile (P89I) resulted in *d*-camphor bound in both orientations, the "closed-door" orientation driven by Pdx binding as well as the open Pdx-free form.[30,31] We proposed that the *trans*−*cis* isomerization of the Ile88−Pro89 bond is driven by Pdx binding, and the isomerization is the origin of the perturbations observed upon formation of the Pdx^r−CYP complex. Many P450s have an Ile (or Val)−Pro combination at the N-terminus of the B′ helix, suggesting that this isomerization is a common means of controlling active site access.[1] Others have a similar arrangement in the F−G loop, which could serve the same function.[1]

The nature of the complex formed by Pdx and CYP101A1 has continued to be a focus of interest in recent years. Spectroscopic studies have on one hand confirmed that the interaction between the two proteins is redox-dependent,[32] while crystallographic studies differ on whether the open or closed states of CYP101A1 predominate in the complex.[15,16,29] Although CYP−S−CO and CYP−S−O_2 are both in the same oxidation state, they differ in electronic configuration, and the instability of the oxygenated complex precludes direct NMR observation of the complexation of that species with Pdx^r. As such, some open questions remain concerning the precise nature of the complex.

SUBSTRATE-DEPENDENT CONFORMATIONAL CHANGES IN CYP101A1

We next turned our attention to the effects of substrate on CYP101A1 conformational selection. We found that removal of substrate or replacement by substrate analogs affected multiple regions of the enzyme, including the I helix adjacent to the active site and the C−D loop on the proximal side of the enzyme. One surprising set of changes was observed in the K′ helix (Figure 4).[33] The K′ helix is a short helix that connects the *β*-meander (which includes the axial heme thiolate ligand) to the *β*3 sheet bordering the active site. While residues in the *β*3 sheet show little change upon substrate binding, amides in the K′ helix show relatively large perturbations, even though the K′ residue nearest to the active site, Ser325, is ∼14 Å from bound substrate. We proposed that the K′ helix (which is highly conserved across the P450 superfamily) adjusts the position of the *β*3 sheet in response to substrate binding by changing hydrogen bonding patterns from that of an *α*-helix to that of a 3-10 helix (Figure 4). This changes the length of the K′ helix, moving the *β*3 sheet as a unit in response to the presence of substrate.

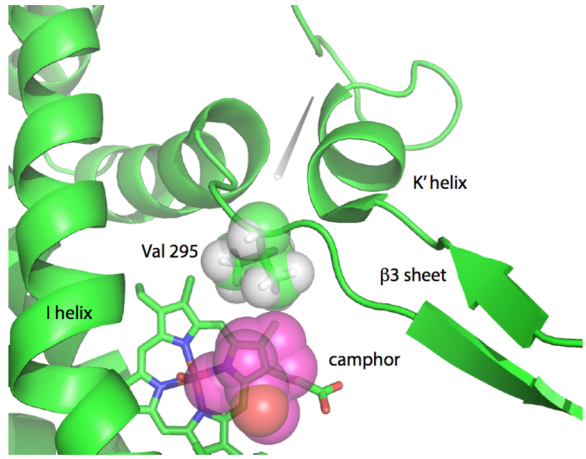

Figure 4. Changing hydrogen bond patterns in the K′ helix of CYP101A1 (PDB entry 2L8M) adjusts the position of substrate contact Val295 (*β*3 sheet) relative to substrate camphor (in purple spheres) by changing the length of the K′ helix. Camphor is in the foreground of the figure, with the heme behind. Direction of helix length adjustment is shown as gray scale arrow parallel to the K′ helix. See text for details.

Solution Structural Ensembles of Substrate-Free and -Bound CYP101A1

While ^{1}H,^{15}N HSQC spectra provide a rapid residue-specific means of localizing responses to events such as substrate or effector binding, the observed spectral changes are responses to changes in hydrogen bond lengths or angles or other local electronic factors rather than conformational changes *per se*. In order to visualize the structural changes causing the perturbations, we required direct structural information. This was obtained in the form of residual dipolar couplings (RDCs) measured for backbone amide ^{1}H−^{15}N correlations.

In solution NMR, coherences are transferred via through-bond *J*-couplings that are independent of magnetic field strength. But nuclear spins also interact via through-space (dipolar) coupling. As the interaction between two bar magnets depends upon their relative orientations, so does the sign and magnitude of the dipolar coupling between an amide ^{1}H and ^{15}N depend upon the angle that the internuclear vector makes with respect to the applied field. In isotropic solution, the dipolar coupling averages to zero. However, if a material that aligns in the magnetic field (e.g., phage particles or liquid crystal) is added to the sample, collisions between the aligned additive and protein molecules introduce a slight orientational preference in the molecular tumbling. This preference reintroduces the ^{1}H−^{15}N dipolar coupling in a attenuated form known as a residual dipolar coupling (RDC).[34] RDCs are detected as a modulation of the ^{1}H−^{15}N *J*-coupling, with the sign and magnitude of the RDC dependent upon the average orientation of the N−H bond vector with respect to the applied magnetic field. By fitting measured RDCs to an alignment tensor, possible orientations of the N−H bond in the molecular frame of reference are obtained. RDCs can be used as restraints in molecular dynamics (MD) simulations, a process we call "soft annealing", to provide an ensemble average of the orientations of secondary structures in the molecular frame.

DOI: 10.1021/acs.accounts.9b00066
Acc. Chem. Res. 2019, 52, 1409−1418

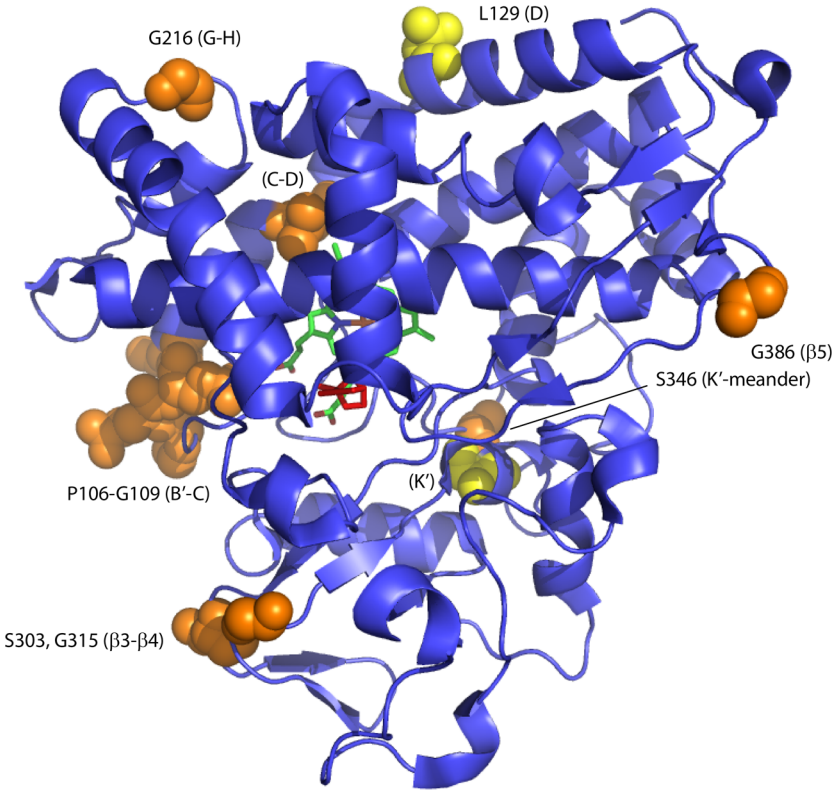

Figure 5. Long-range coupled motions (normal modes) associated with substrate binding and orientation in cytochrome $P450_{cam}$ identified by NMR-directed molecular dynamics simulations, as described in ref 39. Residues highlighted in orange represent the end points of normal modes active when substrate (*d*-camphor, shown in red) is bound, while those in yellow correspond to shorter range motions active in the absence of substrate. Parenthetic labels refer to nearby secondary structures (see Figure 3).

RDCs for CYP101A1 amide N−H pairs measured with and without bound substrate were used as restraints in MD simulations,[35,36] resulting in the first noncrystallographic P450 structures in the PDB (entries 2L8M and 2LQD). Comparison of substrate-free and -bound structures showed some striking conformational shifts. As predicted, hydrogen bonding patterns in the K′ helix change, and this change is linked to an essential collapse of the active site in the absence of substrate, due to inward movements of the β3 sheet and B−B′ loop. Large movements in the C, D loop were seen, as well as a rotation around the long axis of the N-terminal half of the I helix (see Figure 3). This rotation results in changes in the hydrogen bonding pattern in the I helix "kink", a region of irregular hydrogen bonding near the heme that forms the O_2 binding site.[37] We used mutagenesis to confirm that the conformational changes we observed were not artifacts of the methodology but realistic representations of substrate-dependent conformational selection.[38]

Enzyme Control of Regio- and Stereochemistry

An important insight from our NMR-derived structures was that CYP101A1 secondary structures do not fray in the absence of substrate but move as units: Structural reorganization is the result of changes in relative orientations or displacements of secondary structural features when substrate is bound, not local unfolding. This fits with our observation that the biggest substrate-dependent spectral changes are found at junctions between secondary structures (turns and loops) rather than within the structures themselves. To probe the role that motions of secondary structures play in determining the regio- and stereochemistry of the CYP101A1-catalyzed oxidation, Eliana Asciutto at UNSAM/CONICET (Buenos Aires) performed a series of MD simulations starting from 2L8M and 2LQD and analyzed the resulting dynamics tracks using perturbation response scanning (PRS), a means of determining the sensitivity of one region of the protein to structural fluctuations elsewhere.[39] She detected several long-range normal mode displacements that are active in substrate-bound CYP101A1 but inactive in the substrate-free enzyme. These modes lie essentially along the longest diagonals of the P450 structure (Figure 5), implying that the entire enzyme structure is involved in maintaining substrate position, not just those residues contacting substrate in the active site. Conversely, modes active in the absence of substrate are weaker and more localized.

Second, she found that by including a dihedral restraint that rotates substrate away from its preferred orientation relative to the heme plane, dramatically different PRS patterns were obtained. Even changes in the dihedral restraint as small as 10° results in different PRS response patterns (Figure 6). Based on these observations, we conclude that the long-range normal modes activated by substrate binding are critical for determining substrate orientation relative to the active Fe═O complex and enforce the regio- and stereochemistry of the ultimate hydroxylation. These conclusions have obvious implications for rational enzyme engineering, a current area of interest for our group.

CAN WHAT WE LEARN FROM CYP101A1 BE APPLIED TO OTHER P450 ENZYMES?

In many respects, CYP101A1 is an outlier in the P450 superfamily. The requirement for Pdx as an effector is unusually

DOI: 10.1021/acs.accounts.9b00066
Acc. Chem. Res. 2019, 52, 1409−1418

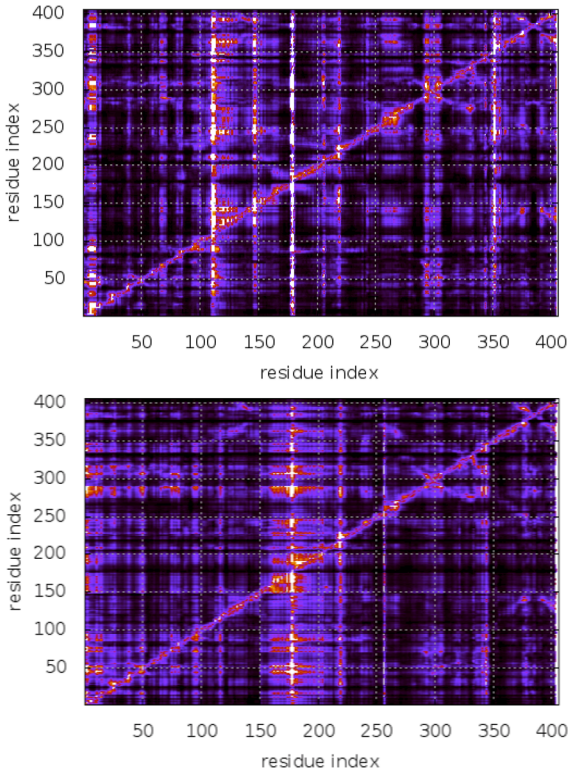

Figure 6. Heat maps showing the sensitivity of perturbation response patterns (normal modes) as a function of amino acid sequence to orientation of substrate *d*-camphor in the active site of CYP101A1. Most sensitive regions are the brightest. Top and bottom maps differ in substrate orientation by 10°. See text and ref 39 for details.

specific: Many P450s exhibit turnover with a noncognate redox partner. The almost complete shift to high spin upon substrate binding observed for CYP101A1 is also atypical, although evidence suggests that all P450s require some degree of high spin formation upon substrate binding,[40] and the effector requirement is, if not universal, quite general. Other observations that we have made along the way (the conserved K′ helix, for example, or the common occurrence of an Xaa−Pro at the N-terminal end of the B′ helix) suggest that there are other commonalities shared among members of the P450 superfamily.

To test whether our conclusions are generalizable to other P450s, we characterized MycG, a P450 from the biosynthetic pathway of mycinamicin II (M-II), a macrolactone antibiotic.[41] MycG is slightly smaller than CYP101A1, (398 vs 414 residues) and sequence identity between CYP101A1 and MycG is low (~23%). Their substrates differ dramatically in structure, size, and hydrophobicity. Furthermore, MycG is bifunctional, catalyzing the last two steps of M-II biosynthesis, a hydroxylation followed by an epoxidation (Figure 7), both of which are regio- and stereoselective.[42] Crystallographic structures of MycG with M-IV bound showed an open active site, with M-IV not suitably oriented for the observed chemistry, so further rearrangements must take place prior to hydroxylation.

After sequential assignment of MycG, RDCs were used to calculate solution structural ensembles for the M-IV-bound enzyme. Paramagnetic ^{1}H relaxation rates were used as distance restraints for M-IV orientation in the active site.[43] Comparison of the MycG crystallographic (PDB entry 2Y98) and RDC-based structures (PDB entry 5UHU) showed that the orientation and placement of substrate M-IV differs drastically between the two. In the crystal, much of the M-IV molecule lies between the F and G helices that form the "cap" of the P450 active site, in an orientation perpendicular to the heme plane, while in solution, M-IV lies roughly parallel to the heme (Figure 8a). The orientation and placement of M-IV between the F and G helices in the crystal is reminiscent of that of an inhibitor, quinidine, in the crystal structure of CYP2D6, a human P450.[44] This leads us to speculate that the crystallographic position of M-IV is an inhibitory binding mode (Figure 8b). High substrate concentrations are inhibitory for many P450 enzymes, including MycG.[43] Binding of M-IV in this mode might inhibit movements of the F−G helix structures necessary for appropriate substrate binding or catalysis. Furthermore, this "locked" conformer may crystallize readily due to its compactness.

CONFORMATIONAL CHANGES UPON SUBSTRATE BINDING IN TWO DIFFERENT P450 ENZYMES

We then went on to characterize solution conformations of substrate-free MycG. Again using RDCs, we compared the conformational changes upon M-IV binding to MycG with those observed for camphor binding to CYP101A1.[45] While some specific differences were noted, those differences can be rationalized in terms of substrate size and coupled motions needed to accommodate substrate. More striking were the similarities: In both cases, changing hydrogen bond patterns in

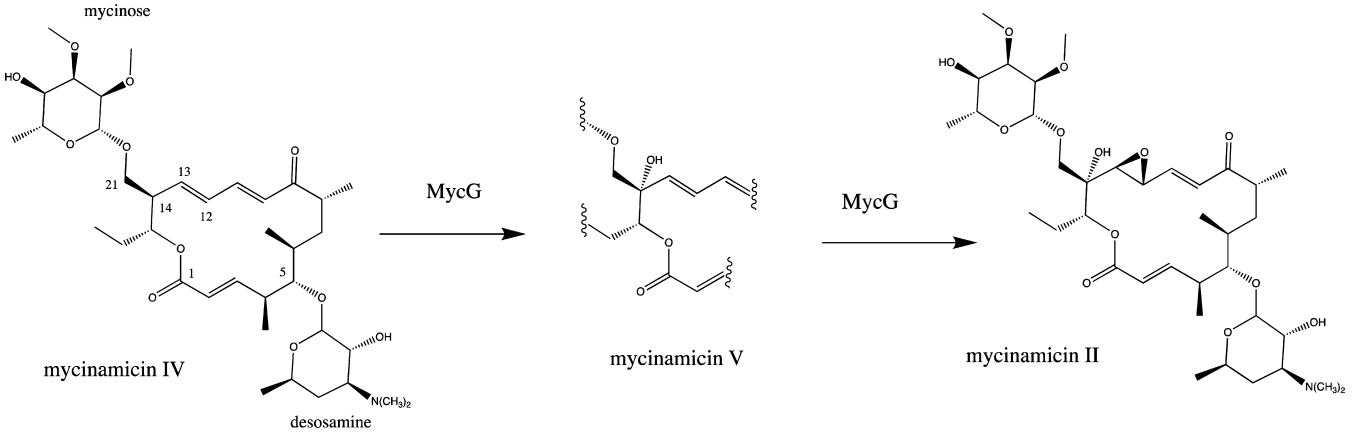

Figure 7. Sequential oxidations catalyzed by MycG in the biosynthesis of mycinamicin II (M-II).

DOI: 10.1021/acs.accounts.9b00066
Acc. Chem. Res. 2019, 52, 1409−1418

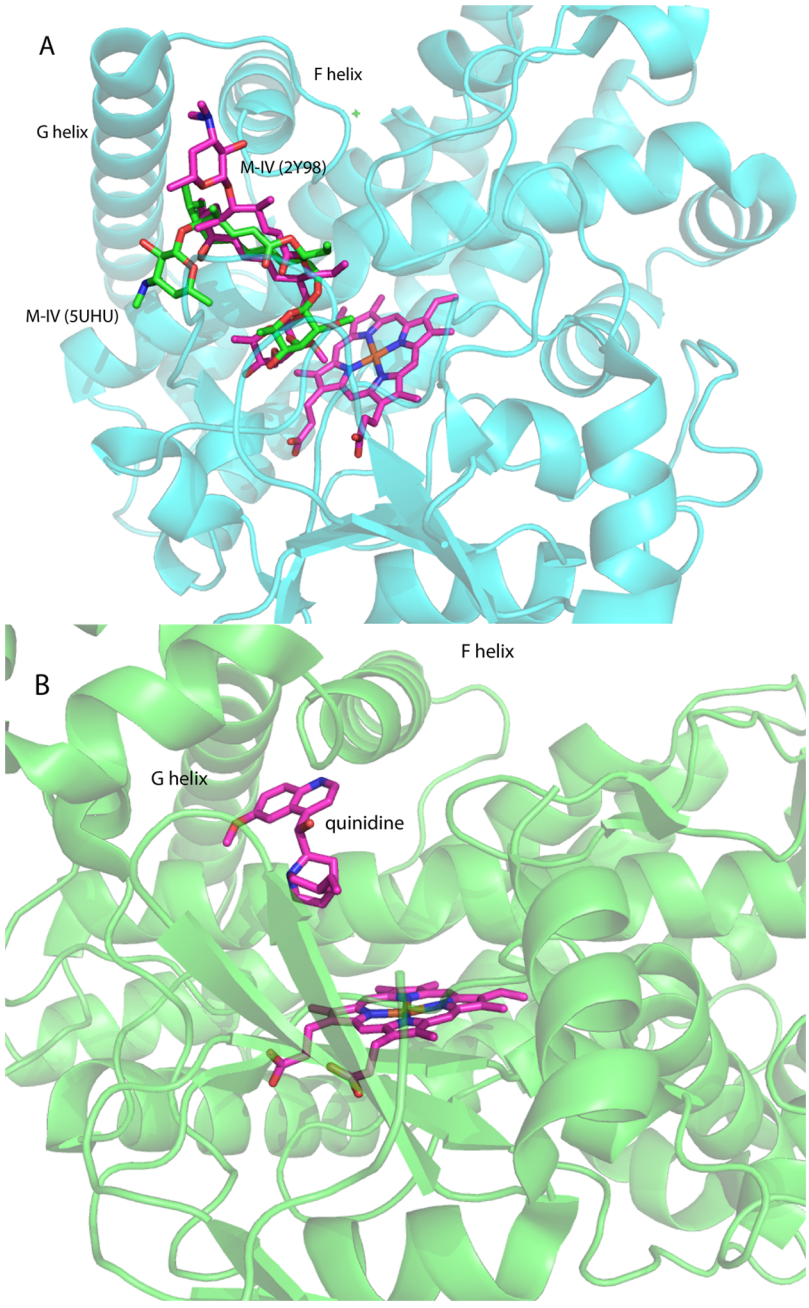

Figure 8. (A) Mycinamycin IV (M-IV) binding modes in the crystallographic (2Y98, purple) and NMR-based structures (5UHU, green). (B) Inhibitor quinidine binding mode in CYP2D6 structure (4WNU).

the K′ helix is critical for modulating the position of the β3 sheet appropriately for substrate contacts in the active site, and overall, the same sense of coordinated displacements of the A and B helices and β-rich regions are seen.

A complementary observation was that the regions *least* perturbed upon substrate binding in both enzymes are the same: these include the J, K, and L helices and the irregular secondary structure (the "β-meander") that contains the axial heme thiolate ligand cysteine residue. Furthermore, while overall sequence homology is low between the two enzymes, homology is highest in the unperturbed regions (63% identity, 78% sequence similarity, and no gaps). The conservation suggests that these regions represent the "core" structural features that must be conserved in order to safely activate molecular oxygen, regardless of substrate.[45]

WHAT'S NEXT? THE MEMBRANE BARRIER AND EUKARYOTIC P450 ENZYMES

The similarities we see between substrate binding in MycG and that in CYP101A1 are suggestive of commonalities in structure/function relationships in the P450 superfamily, but hardly proof. There are over 600 000 genes in GenBank assigned to P450s, and their sheer number is indicative of the multitude of substrate/product combinations that P450 catalysis encompasses. Characterization of even a small fraction of these enzymes is inconceivable. More efficient is to characterize a representative of each class, as determined by substrate–product types. CYP101A1 provides an example of a catabolic enzyme with a small hydrophobic substrate, while MycG binds a large mesophilic substrate as part of a biosynthetic pathway. We are currently investigating another enzyme, $P450_{meg}$

DOI: 10.1021/acs.accounts.9b00066
Acc. Chem. Res. 2019, 52, 1409–1418

(CYP106A2), which hydroxylates steroidal substrates, making this enzyme of interest for drug manufacturing.[46] Furthermore, steroid oxidations are among the roles that P450s play in higher organisms. The elaboration and modification of cholesterol to biosynthesize most steroid hormones involve P450s at some stage. These P450s are targets for chemotherapy in steroid-responsive cancers, and an understanding of how steroidal substrates are bound and oriented in the active sites of the relevant P450s has implications for drug design. We are currently working on several human P450s, including CYP17A1, CYP2D6, and CYP3A4, in collaboration with Emily Scott's group at the University of Michigan. Her group has shown that the human steroidogenic CYP17A1 is amenable to solution NMR,[47,48] and together we have now made ∼50% of the amide backbone N−H assignments for that enzyme.

Eukaryotic P450s present greater challenges than their bacterial counterparts. Heterologous expression of eukaryotic P450s can be difficult, often requiring chaperone coexpression for proper folding. They are usually larger than bacterial P450s, resulting in increased spectral complexity. But, more importantly, eukaryotic P450s contain an N-terminal helical membrane binding domain, and often display hydrophobic residues on their surfaces to facilitate interaction with membranes. This can lead to oligomerization, with concomitant increased molecular weight and shorter coherence lifetimes. Furthermore, it seems likely that active site/membrane interactions are critical for determining active site geometry and substrate orientation.[49] However, with advances such as the use of nanodisc membrane models to facilitate solution NMR examinations of membrane proteins,[50,51] we foresee that these problems can be solved, and NMR will continue to offer further important insights into P450 enzyme structure and dynamics.

It is important to consider the strengths and limitations of any methodology when drawing functional conclusions from a structure. While crystallography offers atomic-level details that no other structural method can match, it should be remembered that even the most detailed still-life portrait can only suggest motion. NMR can fill in some of the gaps and provide a fourth dimension to your enzyme's structure.

AUTHOR INFORMATION

Corresponding Author

*E-mail: pochapsk@brandeis.edu.

ORCID

Thomas C. Pochapsky: 0000-0001-8995-1088

Notes

The authors declare no competing financial interest.

Biographies

Thomas Pochapsky received his Ph.D. degree in organic chemistry from the University of Illinois (UIUC) in 1986, followed by postdoctoral research in biochemistry at Illinois and the Scripps Research Institute (La Jolla, CA). He joined Brandeis University in 1989, where he is a Professor of Chemistry and Biochemistry.

Susan Sondej Pochapsky received her Ph.D. degree in organic chemistry at UIUC in 1988, followed by postdoctoral research at the Scripps Oceanographic Institute in La Jolla. She joined Bruker Instruments as an applications scientist in 1990, later moving to the Bitter Magnet Laboratory at MIT. She came to Brandeis in 2000, where she is currently Director of the Brandeis NMR Facility.

ACKNOWLEDGMENTS

The authors thank the undergraduate, graduate, and postdoctoral researchers and our many collaborators who have contributed to this work over the years. Most of the work described in this Account was supported by NIH Grant R01-GM44191. Current efforts are supported by Grant R01-GM130997.

REFERENCES

(1) Pochapsky, T. C.; Kazanis, S.; Dang, M. Conformational plasticity and structure/function relationships in cytochromes P450. *Antioxid. Redox Signaling* **2010**, *13*, 1273−1296.

(2) Gunsalus, I. C.; Wagner, G. C. Bacterial P450cam methylene monooxygenase components: Cytochrome m, putidaredoxin, and putidaredoxin reductase. *Methods Enzymol.* **1978**, *52*, 166−188.

(3) Poulos, T. L.; Finzel, B. C.; Howard, A. J. High-resolution crystal structure of cytochrome P450cam. *J. Mol. Biol.* **1987**, *195*, 687−700.

(4) Sligar, S. G. Coupling of spin, substrate and redox equilibria in cytochrome P450. *Biochemistry* **1976**, *15*, 5399−5406.

(5) Lipscomb, J. D.; Sligar, S. G.; Namtvedt, M. J.; Gunsalus, I. C. Autooxidation and hydroxylation reactions of oxygenated cytochrome P450cam. *J. Biol. Chem.* **1976**, *251*, 1116−1124.

(6) Pochapsky, T. C.; Ye, X. M. 1H NMR identification of a beta-sheet structure and description of folding topology in putidaredoxin. *Biochemistry* **1991**, *30*, 3850−3856.

(7) Pochapsky, T. C.; Ye, X. M.; Ratnaswamy, G.; Lyons, T. A. An NMR-derived model for the solution structure of oxidized putidaredoxin, a 2-Fe, 2-S ferredoxin from *Pseudomonas*. *Biochemistry* **1994**, *33*, 6424−6432.

(8) Kazanis, S.; Pochapsky, T. C.; Barnhart, T. M.; Penner-Hahn, J. E.; Mirza, U. A.; Chait, B. T. Conversion of a Fe2S2 ferredoxin into a Ga(3+) rubredoxin. *J. Am. Chem. Soc.* **1995**, *117*, 6625−6626.

(9) Kazanis, S.; Pochapsky, T. C. Structural features of the metal binding site and dynamics of gallium putidaredoxin, a diamagnetic derivative of a Cys(4)Fe(2)S(2) ferredoxin. *J. Biomol. NMR* **1997**, *9*, 337−346.

(10) Muller, A.; Muller, J. J.; Muller, Y. A.; Uhlmann, H.; Bernhardt, R.; Heinemann, U. New aspects of electron transfer revealed by the crystal structure of a truncated bovine adrenodoxin, Adx(4−108). *Structure* **1998**, *6*, 269−280.

(11) Nakamura, K.; Horiuchi, T.; Yasukochi, T.; Sekimizu, K.; Hara, T.; Sagara, Y. Significant contribution of arginine 112 and its positive charge of *Pseudomonas putida* cytochrome P450cam in the electron transport from putidaredoxin. *Biochim. Biophys. Acta, Protein Struct. Mol. Enzymol.* **1994**, *1207*, 40−48.

(12) Stayton, P. S.; Sligar, S. G. Structural microheterogeneity of a tryptophan residue required for efficient biological electron transfer between putidaredoxin and cytochrome P450cam. *Biochemistry* **1991**, *30*, 1845−1851.

(13) Pochapsky, T. C.; Lyons, T. A.; Kazanis, S.; Arakaki, T.; Ratnaswamy, G. A structure-based model for cytochrome P450(cam)-putidaredoxin interactions. *Biochimie* **1996**, *78*, 723−733.

(14) Holden, M.; Mayhew, M.; Bunk, D.; Roitberg, A.; Vilker, V. Probing the interactions of putidaredoxin with redox partners in camphor P450 5-monooxygenase by mutagenesis of surface residues. *J. Biol. Chem.* **1997**, *272*, 21720−21725.

(15) Tripathi, S.; Li, H. Y.; Poulos, T. L. Structural basis for effector control and redox partner recognition in cytochrome P450. *Science* **2013**, *340*, 1227−1230.

(16) Hiruma, Y.; Hass, M. A. S.; Kikui, Y.; Liu, W. M.; Olmez, B.; Skinner, S. P.; Blok, A.; Kloosterman, A.; Koteishi, H.; Lohr, F.; Schwalbe, H.; Nojiri, M.; Ubbink, M. The structure of the cytochrome P450cam-putidaredoxin complex determined by paramagnetic NMR spectroscopy and crystallography. *J. Mol. Biol.* **2013**, *425*, 4353−4365.

(17) Pochapsky, T. C.; Ratnaswamy, G.; Patera, A. Redox-dependent 1H NMR spectral features and tertiary structural constraints on the C-terminal region of putidaredoxin. *Biochemistry* **1994**, *33*, 6433−6441.

DOI: 10.1021/acs.accounts.9b00066
Acc. Chem. Res. 2019, 52, 1409−1418

(18) Lyons, T. A.; Ratnaswamy, G.; Pochapsky, T. C. Redox-dependent dynamics of putidaredoxin characterized by amide proton exchange. *Protein Sci.* **1996**, *5*, 627−639.
(19) Jain, N. U.; Pochapsky, T. C. Redox dependence of hyperfine-shifted 13C and 15N resonances in putidaredoxin. *J. Am. Chem. Soc.* **1998**, *120*, 12984−12985.
(20) Pochapsky, T. C.; Kostic, M.; Jain, N.; Pejchal, R. Redox-dependent conformational selection in a Cys(4)Fe(2)S(2) ferredoxin. *Biochemistry* **2001**, *40*, 5602−5614.
(21) Kostic, M.; Pochapsky, S. S.; Obenauer, J.; Mo, H. P.; Pagani, G. M.; Pejchal, R.; Pochapsky, T. C. Comparison of functional domains in vertebrate-type ferredoxins. *Biochemistry* **2002**, *41*, 5978−5989.
(22) Sevrioukova, I. F.; Garcia, C.; Li, H. Y.; Bhaskar, B.; Poulos, T. L. Crystal structure of putidaredoxin, the 2Fe-2S component of the P450cam monooxygenase system from Pseudomonas putida. *J. Mol. Biol.* **2003**, *333*, 377−392.
(23) Sevrioukova, I. F. Redox-dependent structural reorganization in putidaredoxin, a vertebrate-type [2Fe-2S] ferredoxin from Pseudomonas putida. *J. Mol. Biol.* **2005**, *347*, 607−621.
(24) Bax, A.; Grzesiek, S. Methodological advances in protein NMR. *Acc. Chem. Res.* **1993**, *26*, 131−138.
(25) Pochapsky, S. S.; Pochapsky, T. C.; Wei, J. W. A model for effector activity in a highly specific biological electron transfer complex: The cytochrome P450cam−putidaredoxin couple. *Biochemistry* **2003**, *42*, 5649−5656.
(26) Ludemann, S. K.; Lounnas, V.; Wade, R. C. How do substrates enter and products exit the buried active site of cytochrome P450cam? 2. Steered molecular dynamics and adiabatic mapping of substrate pathways. *J. Mol. Biol.* **2000**, *303*, 813−830.
(27) Schlichting, I.; Berendzen, J.; Chu, K.; Stock, A. M.; Maves, S. A.; Benson, D. E.; Sweet, R. M.; Ringe, D.; Petsko, G. A.; Sligar, S. G. The catalytic pathway of cytochrome P450cam at atomic resolution. *Science* **2000**, *287*, 1615−22.
(28) Wei, J. Y.; Pochapsky, T. C.; Pochapsky, S. S. Detection of a high-barrier conformational change in the active site of cytochrome P450cam upon binding of putidaredoxin. *J. Am. Chem. Soc.* **2005**, *127*, 6974−6976.
(29) Follmer, A. H.; Tripathi, S.; Poulos, T. L. Ligand and redox partner binding generates a new conformational state in cytochrome P450cam (CYP101A1). *J. Am. Chem. Soc.* **2019**, *141*, 2678−2683.
(30) OuYang, B.; Pochapsky, S. S.; Dang, M.; Pochapsky, T. C. A functional proline switch in cytochrome P450cam. *Structure* **2008**, *16*, 916−923.
(31) Asciutto, E. K.; Madura, J. D.; Pochapsky, S. S.; OuYang, B.; Pochapsky, T. C. Structural and dynamic implications of an effector-induced backbone amide cis-trans isomerization in cytochrome P450cam. *J. Mol. Biol.* **2009**, *388*, 801−814.
(32) Myers, W. K.; Lee, Y. T.; Britt, R. D.; Goodin, D. B. The conformation of P450cam in complex with putidaredoxin is dependent on oxidation state. *J. Am. Chem. Soc.* **2013**, *135*, 11732−11735.
(33) Dang, M.; Pochapsky, S. S.; Pochapsky, T. C. Spring-loading the active site of cytochrome P450cam. *Metallomics* **2011**, *3*, 339−343.
(34) Prestegard, J. H.; Bougault, C. M.; Kishore, A. I. Residual dipolar couplings in structure determination of biomolecules. *Chem. Rev.* **2004**, *104*, 3519−3540.
(35) Asciutto, E. K.; Dang, M.; Pochapsky, S. S.; Madura, J. D.; Pochapsky, T. C. Experimentally restrained molecular dynamics simulations for characterizing the open states of cytochrome P450cam. *Biochemistry* **2011**, *50*, 1664−1671.
(36) Asciutto, E. K.; Young, M. J.; Madura, J. D.; Pochapsky, S. S.; Pochapsky, T. C. Solution structural ensembles of substrate-free cytochrome P450cam. *Biochemistry* **2012**, *51*, 3383−3393.
(37) Poulos, T. L. Cytochrome P450. *Curr. Opin. Struct. Biol.* **1995**, *5*, 767−774.
(38) Colthart, A. M.; Tietz, D. R.; Ni, Y.; Friedman, J. L.; Dang, M.; Pochapsky, T. C. Detection of substrate-dependent conformational changes in the P450 fold by nuclear magnetic resonance. *Sci. Rep.* **2016**, *6*, 22035.
(39) Asciutto, E. K.; Pochapsky, T. C. Some surprising implications of NMR-directed simulations of substrate recognition and binding by cytochrome P450cam (CYP101A1). *J. Mol. Biol.* **2018**, *430*, 1295−1310.
(40) Pochapsky, T. C.; Wong, N.; Zhuang, Y.; Futcher, J.; Pandelia, M.-E.; Teitz, D. R.; Colthart, A. M. NADH reduction of nitroaromatics as a probe for residual ferric form high-spin in a cytochrome P450. *Biochim. Biophys. Acta, Proteins Proteomics* **2018**, *1866*, 126−133.
(41) Anzai, Y.; Saito, N.; Tanaka, M.; Kinoshita, K.; Koyama, Y.; Kato, F. Organization of the biosynthetic gene cluster for the polyketide macrolide mycinamicin in *Micromonospora griseorubida*. *FEMS Microbiol. Lett.* **2003**, *218*, 135−141.
(42) Li, S. Y.; Tietz, D. R.; Rutaganira, F. U.; Kells, P. M.; Anzai, Y.; Kato, F.; Pochapsky, T. C.; Sherman, D. H.; Podust, L. M. Substrate recognition by the multifunctional cytochrome P450 MycG in mycinamicin hydroxylation and epoxidation reactions. *J. Biol. Chem.* **2012**, *287*, 37880.
(43) Tietz, D. R.; Podust, L. M.; Sherman, D. H.; Pochapsky, T. C. Solution conformations and dynamics of substrate-bound cytochrome P450 MycG. *Biochemistry* **2017**, *56*, 2701−2714.
(44) Wang, A.; Stout, C. D.; Zhang, Q. H.; Johnson, E. F. Contributions of ionic interactions and protein dynamics to cytochrome P450 2D6 (CYP2D6) substrate and inhibitor binding. *J. Biol. Chem.* **2015**, *290*, 5092−5104.
(45) Tietz, D. R.; Colthart, A. M.; Pochapsky, S. S.; Pochapsky, T. C. Substrate recognition by two different P450s: Evidence for conserved roles in a common fold. *Sci. Rep.* **2017**, *7*, 13581.
(46) Bernhardt, R.; Urlacher, V. B. Cytochromes P450 as promising catalysts for biotechnological application: chances and limitations. *Appl. Microbiol. Biotechnol.* **2014**, *98*, 6185−6203.
(47) Estrada, D. F.; Laurence, J. S.; Scott, E. E. Substrate-modulated cytochrome P450 17A1 and cytochrome b5 interactions revealed by NMR. *J. Biol. Chem.* **2013**, *288*, 17008−17018.
(48) Bart, A. G.; Scott, E. E. Structural and functional effects of cytochrome b5 interactions with human cytochrome P450 enzymes. *J. Biol. Chem.* **2017**, *292*, 20818−20833.
(49) Monk, B. C.; Tomasiak, T. M.; Keniya, M. V.; Huschmann, F. U.; Tyndall, J. D. A.; O'Connell, J. D.; Cannon, R. D.; McDonald, J. G.; Rodriguez, A.; Finer-Moore, J. S.; Stroud, R. M. Architecture of a single membrane spanning cytochrome P450 suggests constraints that orient the catalytic domain relative to a bilayer. *Proc. Natl. Acad. Sci. U. S. A.* **2014**, *111*, 3865−3870.
(50) Mazhab-Jafari, M. T.; Marshall, C. B.; Smith, M. J.; Gasmi-Seabrook, G. M. C.; Stathopulos, P. B.; Inagaki, F.; Kay, L. E.; Neel, B. G.; Ikura, M. Oncogenic and RASopathy-associated K-RAS mutations relieve membrane-dependent occlusion of the effector-binding site. *Proc. Natl. Acad. Sci. U. S. A.* **2015**, *112*, 6625−6630.
(51) Nath, A.; Atkins, W. M.; Sligar, S. G. Applications of phospholipid bilayer nanodiscs in the study of membranes and membrane proteins. *Biochemistry* **2007**, *46*, 2059−2069.

DOI: 10.1021/acs.accounts.9b00066
Acc. Chem. Res. 2019, 52, 1409−1418